

Full Length Research Paper

Inhibition effect of 1, 2, 3-benzotriazole on the corrosion of aluminium

Akhenaten Al-Fayed and Hatshepsut al-Aqqad*

Department of Chemistry, Faculty of Science, Mansoura University, Mansoura-35516, Mansoura, Egypt.

Accepted 10 December, 2016

The inhibition effect of 1, 2, 3-benzotriazole on the corrosion of aluminium in 0.5 M HCl solution was studied by potentiodynamic polarization, electrochemical impedance spectroscopy (EIS) electrochemical frequency modulation (EFM) methods. The results show that 1, 2, 3-benzotriazole is a good inhibitor at different concentrations. Polarization curves reveal that inhibitor behaves as mixed-type inhibitor. EIS spectra indicated that the addition of inhibitor increases the charge-transfer resistance of the corrosion process, and hence the inhibition performance improved. Results obtained from EFM method are shown to be in agreement with potentiodynamic and EIS methods. The adsorption of 1, 2, 3-benzotriazole on aluminium surface obeys Frumkin adsorption isotherm. Scanning electron microscopy (SEM) analysis was performed to characterize the film formed on the surface of metal. The reactivity of inhibitor was performed through quantum chemical calculations based on DFT method to support the experimental data with the molecular structure of inhibitor.

Key words: Aluminium, polarization, electrochemical impedance spectroscopy (EIS), electrochemical frequency modulation (EFM), scanning electron microscopy (SEM), DFT calculations.

INTRODUCTION

Aluminum has a remarkable economic, industrial importance and attractive material for engineering applications owing to its high thermal and electrical conductivity, low cost and light weight. The resistance of aluminum against corrosion in aqueous media can be attributed to a rapidly formed compact, strongly adherent invisible protective oxide film on its surface (Sastri et al., 2007; Ali and Foad, 2012). Therefore, aluminum has been known to exhibit widely different electrochemical properties in different aqueous electrolytes, such that aluminum and its alloys are widely used in many industries such as food containers, chemical batteries, pipes and reaction vessels. The chemical dissolution and electro plating are the main processes used in the fabrication of electronic devices. The most widely used HCl acid solution is this medium which has induced a great deal of research on aluminium (Abiola et al., 2009; Noor, 2009; Rethinnagiri et al., 2012; Awad et al., 2014). So, the best method for metal protection from corrosion is the use of effective organic inhibitor containing hetero atoms such as (N, O, and S) or structures containing π -electrons in their molecules through which they can

absorb on the metal surface (Dugdale and Cotton, 1963; Bentiss et al., 1999; Khadom et al., 2010; Fares et al., 2012; Frignani et al., 2005; Şafaket al., 2012; El Haleem et al., 2013; Obot et al., 2013; Awad et al., 2014; Li et al., 2014; Manivel et al., 2014). Generally, the adsorption of this inhibitor on a metal surface depends on the nature and surface charge of the adsorbent, the chemical structure of the adsorbate and the type of electrolyte solution (Khaled, 2011). Physisorption and chemisorption are the principal types of interaction between adsorbate and adsorbent. The first one is weak undirected interaction and it is the result of electrostatic attractive forces between inhibiting organic ions or dipoles and electrically charged metal surface. Physisorption involves rapid interaction between adsorbent and adsorbate but it is also easily removed from surface with the temperature increase. In the chemisorption, strong, directed forces

*Corresponding author. E-mail: Hatshepsut2015@gmail.com

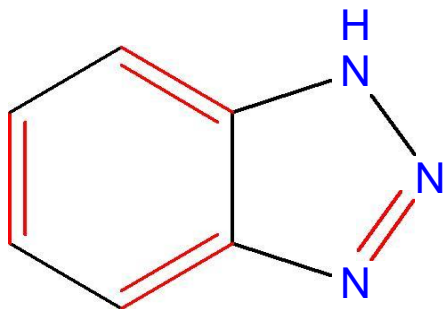


Figure 1. Chemical molecular structure of 1, 2, 3-benzotriazole.

govern the interaction between adsorbate and adsorbent and involve charge sharing or charge transfer from the adsorbate to the adsorbent in order to form a coordinate type of bond (Rozendeld, 1981). Adsorption process can be described by several adsorption isotherms such as: Langmuir, Freundlich, Temkin and Frumkin (Khamis et al., 1991). In the present study, 1, 2, 3-benzotriazole inhibitor was used for corrosion inhibition of aluminium in 0.5 M HCl using potentiodynamic polarization, electrochemical impedance spectroscopy (EIS) and electrochemical frequency modulation (EFM) methods. In addition, SEM processes results are reported and discussed. Quantum chemical calculations were performed to discuss the molecular structure and the reaction mechanisms in order to interpret the experimental results as well as to correlate the inhibition efficiency to the molecular properties of the inhibitor.

EXPERIMENTAL

The working electrode employed in this work was made of pure aluminium (99.99%) supplied by Sigma–Aldrich. For electrochemical measurements, the investigated materials cut as cylindrical rods, welded with Cu-wire for electrical connection and mounted into glass tubes of appropriate diameter using Araldite to offer an active flat disc shaped surface of (0.5 cm²) geometric area, to contact the test solution. Prior to each experiment, the exposed area of the aluminum electrode was abraded with 800, 1200, 1500 and 2000 grades of emery papers. The electrode was then rinsed with acetone, distilled water, and finally dipped in the electrolytic cell. The electrochemical measurements were performed in a typical three-compartment glass cell consisting of the aluminum specimen as working electrode (WE), platinum counter electrode (CE) and a saturated calomel electrode (SCE) as the reference electrode. The electrochemical experiments were performed using a Gamry PCI4G750 Potentiostat/Galvanostat/ZRA analyzer, with a Gamry framework system based on ESA400 connected to a personal computer. Gamry applications include dc105 for dc corrosion measurements, EIS300 for EIS measurements

and EFM140 for EFM measurements along with a computer for collecting data. Echem Analyst 5.5 software was used for plotting, graphing and fitting data. Each run was carried out in aerated solutions at the required temperature, using a water thermostat. All potentials given in this work are referred to this reference electrode (SCE). The electrode was immersed in test solution at open circuit potential (OCP) for 30 min at 30°C before starting the measurements to be sufficient to attain a stable state. The potential of potentiodynamic polarization curves was started from a potential of -250 mV to +250 mV versus OCP at a sweep rate of 0.5 mV s⁻¹. Electrochemical impedance spectroscopy (EIS) was carried out at OCP in the frequency range of 10 mHz – 100 kHz using a 10 mV peak-to-peak sine wave voltages. EFM was carried out using two frequencies of 2.0 and 5.0 Hz. The base frequency was 1.0 Hz. We used a perturbation signal with amplitude of 10 mV for both perturbation frequencies of 2.0 and 5.0 Hz (El-Haddad, 2014; Khadom et al., 2010).

The electrolyte solution of 0.5 M HCl was prepared by dilution of analytical grade 37% HCl with distilled water. Figure 1 shows the molecular chemical structure of 1, 2, 3-benzotriazole inhibitor which was obtained from Sigma–Aldrich Company. The concentration range of inhibitor was 0.3×10^{-4} - 1.8×10^{-4} M.

The scanning electron microscopy (SEM) analysis for the surface characterization of Al specimens were performed with (SEM, JOEL, JSM-T20, Japan). Prior to analysis, the Al specimens were immersed in 0.5 M HCl solutions with/without addition of 1.8×10^{-4} M of inhibitor at 30°C for 24 h. After that, the specimens were cleaned with distilled water, dried with a cold air, and then examined.

Quantum chemical calculations

Quantum chemical calculations were performed with *DMol³* numerical DFT in Materials Studio 5.0 software (Clark et al., 2009). DFT semi-core pseudopotentials calculations (dspp) were performed with the double numerical basis sets plus polarization functional (DNP) to obtain the geometrical optimization of inhibitor, then the molecule's frontier orbital was expressed as relative density distribution figure. *DMol³* includes certain COSMO controls which allow for the treatment of solvation effects (Lee et al., 1988). So, the quantum calculations for inhibitor were performed in a protonated form in acid solution.

RESULTS AND DISCUSSION

Potentiodynamic polarization measurement

The polarization behavior of aluminium electrode in 0.5 M HCl solutions in the absence and presence of different concentrations of 1, 2, 3-benzotriazole at 30°C are

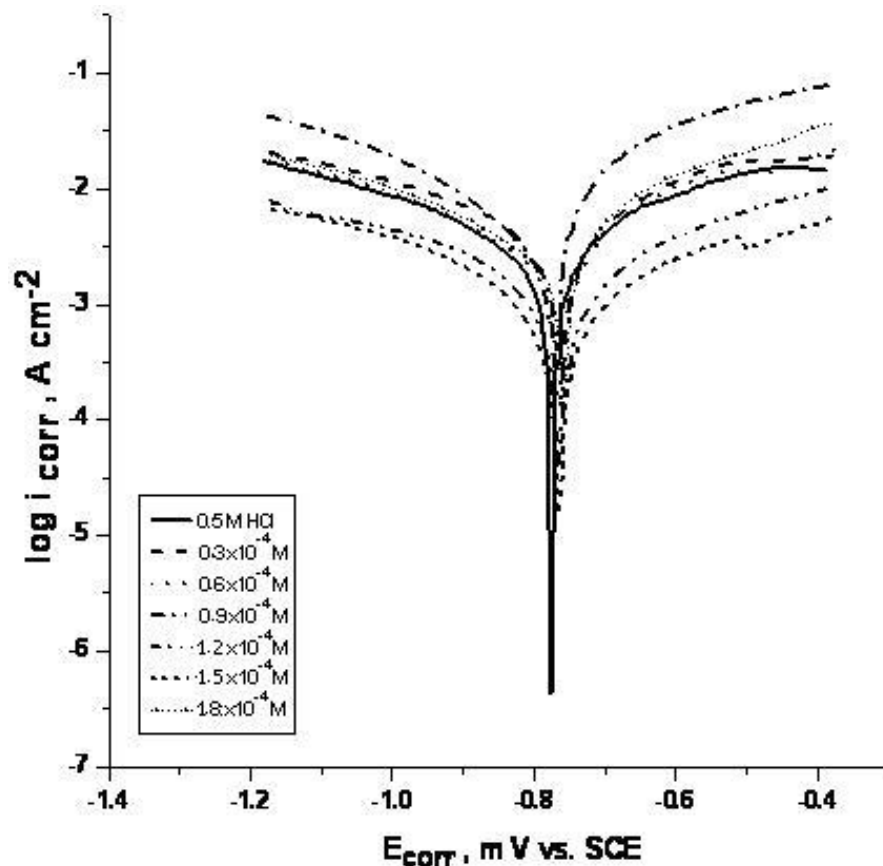


Figure 2. Potentiodynamic polarization curves for the corrosion of aluminum in 0.5 M HCl in absence and presence of different concentrations of 1, 2, 3-benzotriazole at 30°C.

presented in Figure 2. It is clear that the anodic and cathodic reactions are affected by the inhibitor. Based on this result, 1, 2, 3-benzotriazole inhibits corrosion by controlling both anodic and cathodic reactions (mixed-type inhibitors).

The measured free corrosion potential used for this study was found to be -776 mV for aluminum in 0.5 M HCl. Li et al. (2014) found that the free corrosion potential for aluminum in 1.0 M HCl is -785.1 mV, El-Deeb et al. (2013) found the free corrosion potential for aluminum in 0.05 M HCl as -820 mV, and Abd El Wanees et al. (2013) found it to be -980 mV for aluminum in 2.0 M HCl. From these results, one can conclude that the free corrosion potential depends on both the composition of the electrode and the concentration of electrolyte used. The electrochemical parameters including corrosion current densities (i_{corr}), corrosion potential (E_{corr}), cathodic and anodic Tafel slopes (β_c and β_b) and corresponding inhibition efficiency ($\%IE_{pp}$) associated with polarization measurements of 1, 2, 3-benzotriazole at different concentrations were determined and listed in Table 1. The inhibition efficiency ($\%IE_{pp}$) and surface coverage (θ)

were calculated according to the following equations (Foudaet al., 2013):

$$\%IE_{pp} = \left[\frac{i_b - i_{inh}}{i_b} \right] \times 100 \quad (1)$$

$$\theta = \left[\frac{i_b - i_{inh}}{i_b} \right] \quad (2)$$

Where i_b and i_{inh} are the corrosion current densities in the absence and the presence of the inhibitor, respectively. It is clear that i_{corr} decreases with increasing the inhibitor concentration, due to the increase in the blocked fraction of the electrode surface by adsorption (Li et al., 2014).

Electrochemical impedance spectroscopy measurements

Figure 3 shows Nyquist plots of aluminium in 0.5 HCl in the absence and presence of different concentrations of 1, 2, 3-benzotriazole inhibitor at 30°C. The impedance

Table 1. Potentiodynamic polarization parameters for the corrosion of aluminium in 0.5 M HCl containing different concentrations of 1, 2, 3-benzotriazole at 30°C.

Inhibitor Conc., M	-E _{corr} , mV	i _{corr} , μA cm ⁻²	β _c , mV dec ⁻¹	β _a , mV dec ⁻¹	θ	%I _{Epp}
0	776	593	303	246	---	---
0.3 × 10 ⁻⁴	766	536	300	282	0.096	9.6
0.6 × 10 ⁻⁴	764	424	315	207	0.286	28.6
0.9 × 10 ⁻⁴	772	299	315	220	0.496	49.6
1.2 × 10 ⁻⁴	765	216	327	233	0.635	63.5
1.5 × 10 ⁻⁴	764	150	329	262	0.747	74.7
1.8 × 10 ⁻⁴	759	130	336	253	0.782	78.2

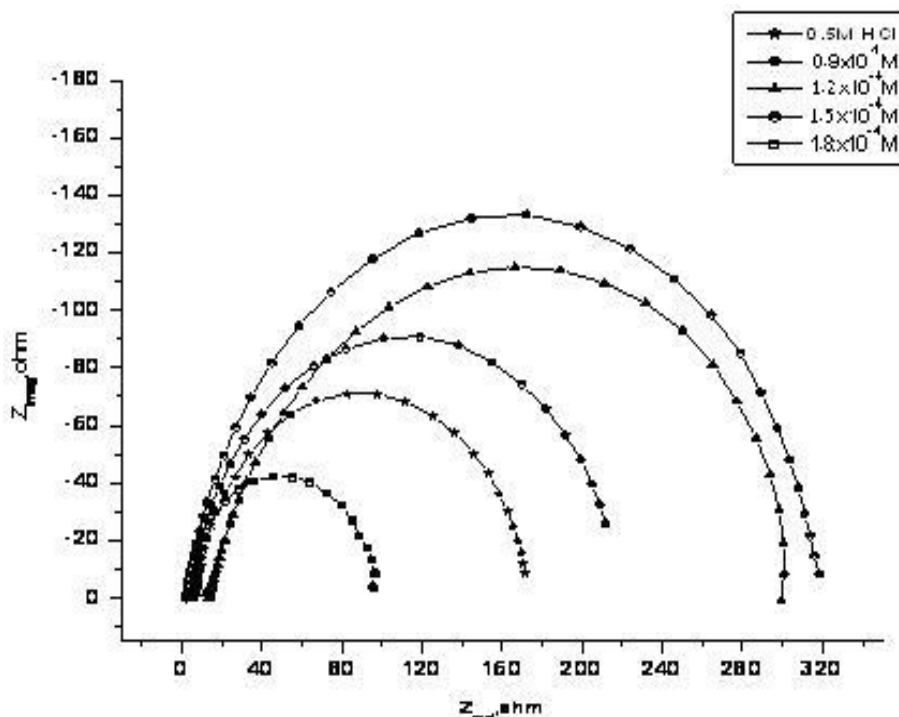


Figure 3. The Nyquist plot for aluminium electrode in 0.5 M HCl solution in the absence and presence of different concentrations of 1, 2, 3-benzotriazole at 30°C.

spectra exhibit one single depressed semicircle, and the diameter of semicircle increases with increasing inhibitor concentration. The single semicircle indicates that the charge transfer takes place at electrode/solution interface, and the corrosion reaction of Al is controlled by the transfer process (Larabi et al., 2004). The experimental data fitted using the electrical equivalent circuit, which are given in Figure 4. In this circuit, R_s and R_{ct} represent the solution resistance between the steel electrode and the reference electrode and the charge-transfer resistance corresponding with the corrosion reaction at metal substrate/solution interface, respectively. The capacity of double layer C_{dl} is defined as:

$$C_{dl} = \frac{1}{2\pi \int_{max}^{ct} R} \tag{3}$$

Where f_{max} is the maximum frequency at which imaginary value reaches a maximum on the Nyquist plot.

The inhibition efficiencies (%I_{EIS}) and the surface coverage (θ) obtained from the impedance measurements are defined by the following relations:

$$\%I_{EIS} = \left| \frac{R_{ct} - R_{ct}^0}{R_{ct}} \right| \times 100 \tag{4}$$

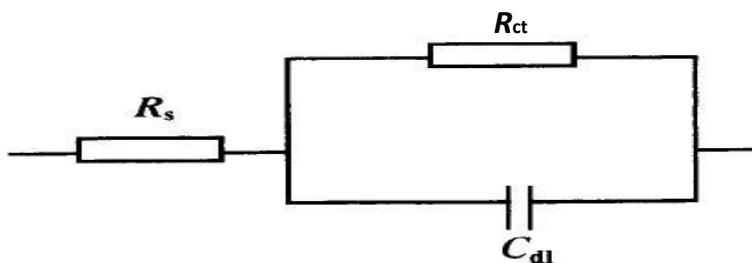


Figure 4. The equivalent circuit model used to fit the experimental results.

Table 2. Electrochemical kinetic parameters obtained by EIS measurement for aluminium in absence and presence of different concentrations of 1, 2, 3-benzotriazole at 30°C.

Inhibitor Conc., M	$R_{ct}, \Omega \text{ cm}^2(A)$	$C_{dl}, \mu\text{F cm}^{-2}$	θ	%IEIS
0	98.47	87.57	-----	-----
0.9×10^{-4}	202.6	88.75	0.514	51.4
1.2×10^{-4}	238.2	78.75	0.587	58.7
1.5×10^{-4}	282.6	72.44	0.652	65.2
1.8×10^{-4}	341.7	57.43	0.712	71.2

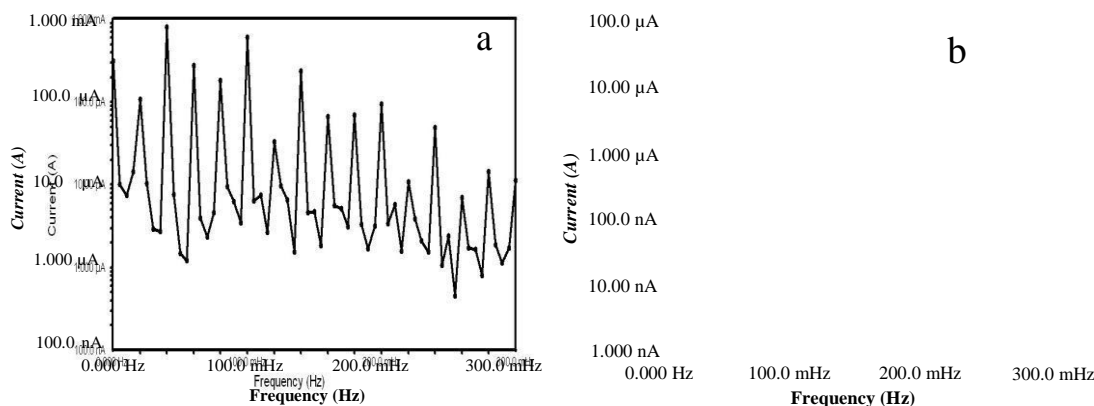


Figure 5. (a) Intermodulation spectrum for aluminium 0.5 M HCl alone at 30°C, and (b) intermodulation spectra for Al in 0.5 M HCl containing 1.8×10^{-4} M of 1, 2, 3-benzotriazole at 30°C.

$$\theta = \left| \frac{R_{ct} - R_{ct}^0}{R_{ct}} \right|$$

Where R_{ct}^0 and R_{ct} are the charge transfer resistance in the absence and presence of inhibitor respectively. Table 2 collects the fitting results recorded from EIS measurements. Data reveal that the charge-transfer resistance (R_{ct}) increases with increase in inhibitor concentration, suggesting the formation of a protective layer on aluminium electrode surface. This layer makes a barrier charge transfer, which causes an increase of %IEIS. At the same time, the double layer capacitance

(C_{dl}) has opposite trend at the whole concentration range.

This is due to decrease in local dielectric constant and increase in thickness of the electrical double layer, suggesting that inhibitor molecules inhibit the metal corrosion via adsorption at the metal/solution interface (El-Haddad and Fouda, 2013).

Electrochemical frequency modulation (EFM)

Intermodulation spectra obtained from EFM measurements for aluminium corrosion in 0.5 M HCl solution without and with (1.8×10^{-4} M) of 1, 2, 3-benzotriazole inhibitor at 30°C is presented in Figure 5.

Table 3. Electrochemical kinetic parameters obtained by EFM measurement for aluminium in absence and presence of different concentrations of 1, 2, 3-benzotriazole at 30°C.

Inhibitor Conc., M	i_{corr} , $\mu\text{A cm}^{-2}$	β_c , mV dec^{-1}	β_a , mV dec^{-1}	CF-2	CF-3	θ	%IE _{EFM}
0	535	113	32	1.8	3.2	-----	-----
0.9×10^{-4}	249	93	24	1.98	2.96	0.535	53.5
1.2×10^{-4}	192	105	38	1.94	3.08	0.642	64.2
1.5×10^{-4}	186	115	45	1.96	3.22	0.653	65.3
1.8×10^{-4}	156	119	59	1.67	3.21	0.709	70.9

The similar results were recorded for the other inhibitor concentrations.

The inhibition efficiency (% E_{EFM}) and the degree of surface coverage (θ) can be calculated from the following equations:

$$\left[\frac{i_b - i_{inh}}{i_{EFM}} \right]_{i=100} \quad (6)$$

$$\theta = \frac{\left[\frac{i_b - i_{inh}}{i} \right]}{\left[\frac{i_b}{b} \right]} \quad (7)$$

The calculated electrochemical parameters (i_{corr} , β_a , β_c , CF-2 and CF-3) are given in Table 3. Inspections of these data infer that the values of causality factors (CF-2 and CF-3) obtained under different experimental conditions are approximately equal to the theoretical values (2 and 3) indicating that the measured data are of good quality (El-Haddad et al., 2013). Addition of increasing concentration of inhibitors to HCl solution decreases the corrosion current density (i_{corr}) more than in blank solution indicating that the inhibitors inhibit the corrosion of Al electrodes in HCl solution through adsorption on its surface (El-Haddad, 2013). The values of β_a and β_c are not changed significantly with increasing the concentration of the inhibitor. This confirms that the presence of this inhibitor does not change the mechanism of the corrosion process.

Adsorption isotherm and standard adsorption free energy (ΔG°_{ads})

In order to get more information about the mode of adsorption of 1, 2, 3-benzotriazole inhibitor on the surface of aluminium at different concentrations of inhibitor, the data obtained from polarization curves have been tested with several adsorption isotherms including Langmuir, Freundlich, Temkin and Frumkin. "Frumkin" adsorption isotherms were found to fit well with the experimental data (Manohar et al., 2006; El-Sayed et al., 2010). The adsorption isotherm relationship of Frumkin is represented by the following equations:

$$\left[\frac{\theta}{(1-\theta)} \right] \exp(-2a\theta) = KC \quad (8)$$

or its linear form:

$$\left[\frac{\theta}{(1-\theta)C} \right]_{i=\ln K - 2a\theta} \quad (9)$$

Where (θ) is the surface coverage, (C) is the inhibitor concentration in the bulk of solution, (a) is the lateral interaction term describing the molecular interactions in the adsorption layer and the heterogeneity of the surface (it is a measure for the steepness of the adsorption isotherms) and (K) is the equilibrium constant of the adsorption reaction. Plotting of θ against $\log C$ resulted to a S-shape curve and is represented in Figure 6a. This is indicating that the adsorption of inhibitor follows Frumkin isotherm. On the other hand, by plotting $\ln [\theta/(1-\theta)C]$ versus θ for Al in 0.5 M HCl containing various concentrations of inhibitor, straight lines were shown and represented in Figure 6b. The linear fitting slope for the Frumkin isotherm gave the value of (a) which equals 1.26 and the intercepts gave the value of (K) which equals 2.9936 M^{-1} for the investigated inhibitor. Legreneee et al. (2002) reported that the higher K value ($>100 \text{ M}^{-1}$) indicates the formation of the stronger and more stable adsorbed layer which is the result of the higher inhibition efficiency. Also the positive values of (a) imply that the interaction between molecules causes an increase in the adsorption energy with the increase of (θ).

K is related to the standard free energy of adsorption (ΔG°_{ads}) as shown in the following equation (El-Haddad and Fouda, 2013):

$$K = \frac{1}{55.5} \exp \left(- \frac{\Delta G^\circ_{ads}}{RT} \right) \quad (10)$$

Where K is the value of 55.5 being the concentration of water in solution expressed in mol, R is the universal gas constant and T is the absolute temperature.

It can be observed that the value of ΔG°_{ads} for 1, 2, 3-benzotriazole inhibitor is negative. Actually, this value is

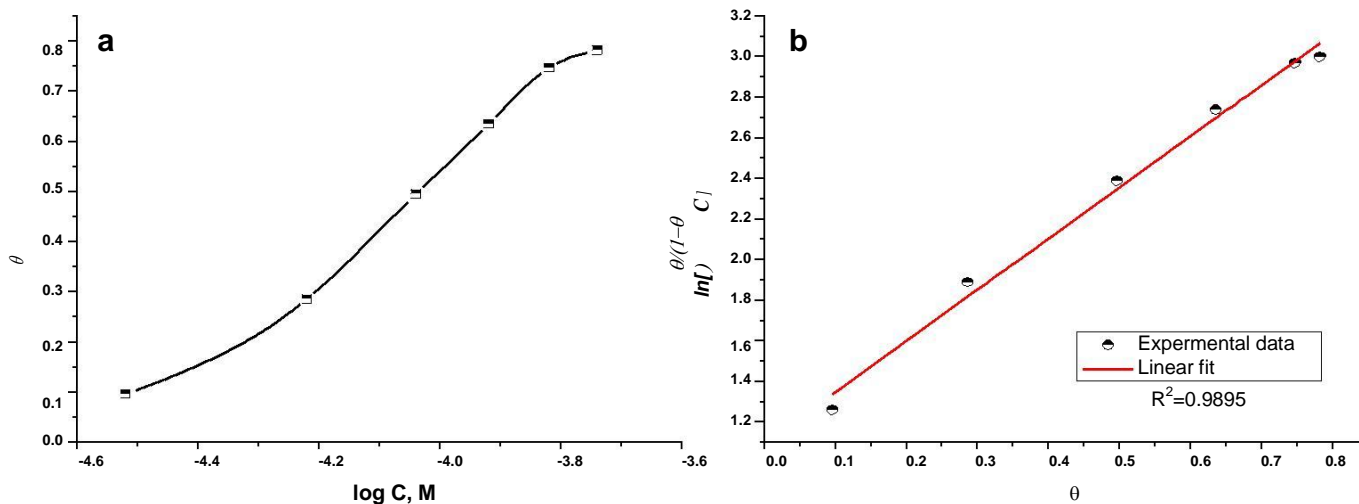


Figure 6. (a) Frumkin adsorption isotherm of investigated 1, 2, 3-benzotriazole on aluminium surface in 0.5 M HCl solution at 30°C. (b) The linear form of Frumkin adsorption isotherm.

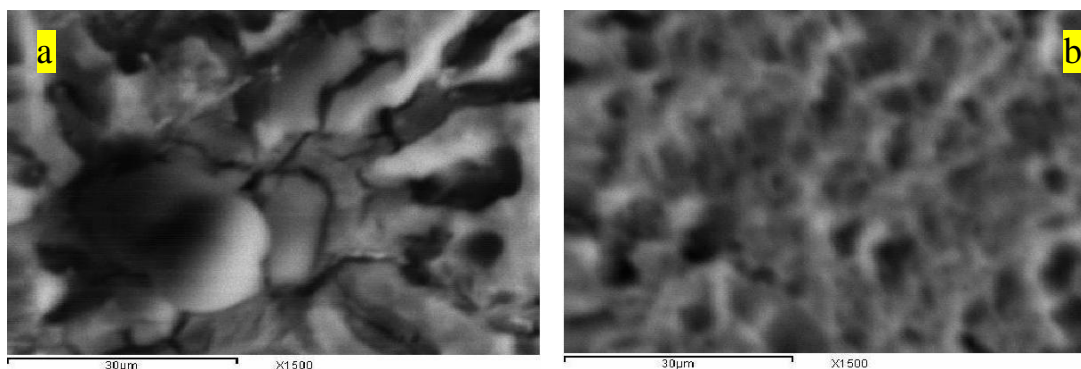


Figure 7. (a) SEM micrographs for aluminium's absence for one day at 30°C, and (b) presence of 1.8×10^{-4} M of 1, 2, 3-benzotriazole for one day at 30°C.

consistent with the spontaneity of the adsorption process and the stability of the adsorbed layer on aluminium surface. It is known that the values of $\Delta G^{\circ}_{\text{ads}}$ of the order -20 kJ mol^{-1} or lower indicate a physisorption, those of the order -40 kJ mol^{-1} or higher involve charge sharing or a transfer from the inhibitor molecules to the metal surface to form a coordinate type of bond, chemisorptions (Hosseini et al., 2003). The value of $\Delta G^{\circ}_{\text{ads}}$ of the investigated 1, 2, 3-benzotriazole was $-12.9 \text{ kJ mol}^{-1}$ at 30°C. This indicates that the adsorption of the investigated 1, 2, 3-benzotriazole on aluminium surface is typical physisorption.

SEM and EDX characterization

Figure 7a represents the SEM obtained of aluminium after exposure to 0.5 M HCl for one day immersion. It is

clear that it suffers from severe corrosion attack. Figure 7b reveals the surface on aluminium after exposure to 0.5 M HCl solution containing 1.8×10^{-4} M of 1, 2, 3-benzotriazole inhibitor. It is important to stress out that when the compound is present in the solution, the morphology of aluminium is quite different from the previous one, and the specimen surface is smoother. One noted the formation of a film which is distributed in a random way on the whole surface of the aluminium. This may be interpreted due to the adsorption of the inhibitor on the aluminium surface incorporating into the passive film in order to block the active site present on the aluminium surface, or due to the involvement of inhibitor molecules in the interaction with the reaction sites of aluminium surface, resulting in a decrease in the contact between aluminium and the aggressive medium and sequentially exhibited excellent inhibition effect

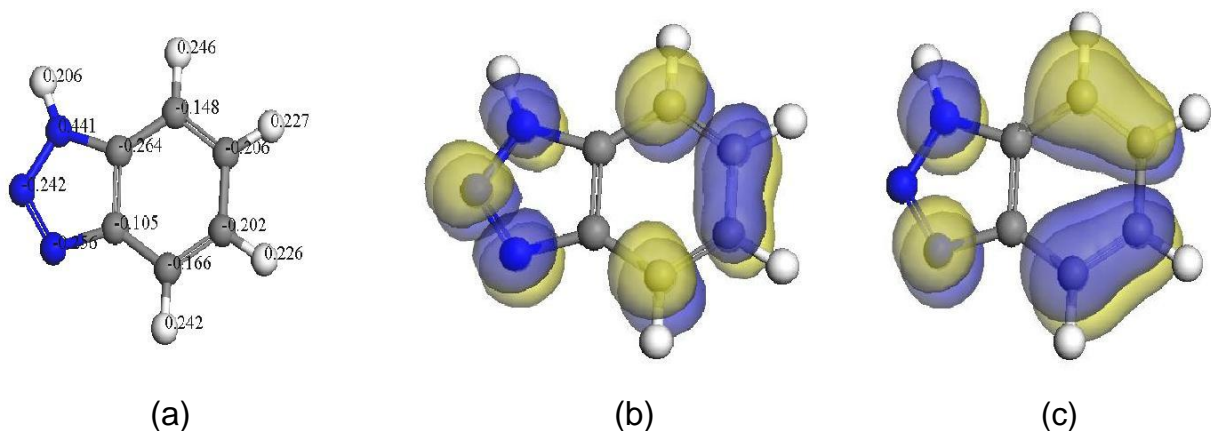


Figure 8. (a) The optimized molecular structure for protonated form of 1, 2, 3-benzotriazole, (b) electronic orbital density distributions of HOMO for protonated form of 1, 2, 3-benzotriazole, and (c) LUMO for protonated form of 1, 2, 3-benzotriazole.

(Muralidharan et al., 1995).

Quantum chemical calculations

Several researchers often used the theoretical data in their studies not only to support their experimental data but also to find the efficient way to minimize the chemical expenditures. So, quantum chemical calculations for protonated form of inhibitor in acidic solution were carried out. Figure 8 shows the optimized molecular structure, electronic orbital density distributions of HOMO and LUMO for protonated form of 1, 2, 3-benzotriazole inhibitor. From the optimized structure of the inhibitor, Milliken charges on the backbone atoms were determined. By comparison of the Milliken charges of atoms for inhibitor, the larger negative atom is found in N atoms (Figure 8), which are active adsorptive atoms. Therefore, these atoms act as an electronic donor, and there is an electrostatic attraction between the metal surface and the investigated inhibitor molecules (El-Haddad and Elattar, 2013). The global reactivity of a molecule depends on molecular distributions. HOMO is often associated with the capacity of a molecule to donate electrons, whereas LUMO represents the ability of the molecule to accept electrons. As shown in Figure 8, HOMO and LUMO are localized on C-N=N-N-H. This indicates that the characteristic functional group of C-N=N-N-H could be both the acceptor of the electron and the donor of the electron. That is, there is electron transferring in the interaction between the C-N=N-N-H and metal surface. High value of E_{HOMO} (-9.402 eV) indicates a tendency of the molecule to donate electrons to act with acceptor molecules with low-energy, empty molecular orbital. Conversely, the E_{LUMO} represents the ability of the molecule to accept electrons, and the lower value of E_{LUMO} (-0.846 eV) suggests the molecule accepts electrons more probable. Low value of the energy gap

$\Delta E = E_{\text{LUMO}} - E_{\text{HOMO}}$ (8.556 eV) will increase the reactivity of molecules, which facilitates adsorption of inhibitor on metal surface. Therefore, it gives good inhibition efficiencies, because the excitation energy to remove an electron from the last occupied orbital will be low (El-Haddad and Elattar, 2013; Li et al., 2009).

Mechanism of corrosion inhibition

The adsorption of the investigated compound can be attributed to the presence of polar unit having atoms of nitrogen and aromatic/heterocyclic rings. Therefore, the possible reaction centers are unshared electron pair of hetero-atoms and π -electrons of aromatic ring (Ahamad et al., 2010). The adsorption and inhibition effect of investigated compound in 0.5 M HCl solution can be explained as follows: In aqueous acidic solutions, 1,2,3-benzotriazole exists either as neutral molecules or as protonated molecules and may adsorb on the metal/acid solution interface by one and/or more of the following ways: (i) electrostatic interaction of protonated molecules with already adsorbed chloride ions, (ii) donor-acceptor interactions between the π -electrons of aromatic ring and vacant p-orbital of surface aluminium atoms, (iii) interaction between unshared electron pairs of hetero-atoms and vacant p-orbital of aluminium surface atoms. In general, two modes of adsorption are considered on the metal surface in acid media. In the first mode, the neutral molecules may be adsorbed on the surface of aluminium through the chemisorption mechanism, involving the displacement of water molecules from the aluminium surface and the sharing electrons between the hetero-atoms and aluminium. The inhibitor molecules can also adsorb on the aluminium surface on the basis of donor-acceptor interactions between π -electrons of the aromatic ring and vacant p-orbitals of surface aluminium atoms. In the second mode (this case), since it is known

that the Al surface bears positive charge in acid solution (Yurt et al., 2006; Obot et al., 2009), it is difficult for the protonated molecules to approach the positively charged aluminium surface due to the electrostatic repulsion. Since chloride ions have a smaller degree of hydration, thus they could bring excess negative charges in the vicinity of the interface and favor more adsorption of the positively charged inhibitor molecules, the protonated 1, 2, 3-benzotriazole adsorb through electrostatic interactions between the positively charged molecules and the negatively charged metal surface. Thus, there is a synergism between adsorbed Cl^- ions and protonated 1,2,3-benzotriazole. It can be concluded that the inhibition of aluminium corrosion in 0.5 M HCl is mainly due to the electrostatic interaction. The decrease in inhibition efficiency with rise in temperature supports electrostatic interaction.

Conclusions

The corrosion inhibition of aluminum 1, 2, 3-benzotriazole was studied by electrochemical measurements and SEM analysis and the obtained results show that:

The inhibition efficiency of 1, 2, 3-benzotriazole in 0.5 M HCl solution increases with increasing its concentration. The inhibitor acts as mixed-type inhibitor. The adsorption of the inhibitor obeys the Frumkin adsorption isotherms. In this study, the calculated value of $\Delta G_{\text{ads}}^{\circ}$ indicated that the adsorption of inhibitor molecules on the aluminium surface is typical physisorption. SEM surface analysis of aluminum confirms the adsorption of 1, 2, 3-benzotriazole and therefore improve surface of metal. Quantum chemical calculations were performed and showed that, relation between the experimental data with the molecular structure of inhibitor.

REFERENCES

- Abiola OK, Otaigbe J, Kio O (2009). Gossipium hirsutum L. extracts as green corrosion inhibitor for aluminum in NaOH solution. *Corros. Sci.*, 51:1879-1881.
- Ahamad I, Prasad R, Quraishi M (2010). Inhibition of mild steel corrosion in acid solution by Pheniramine drug: Experimental and theoretical study. *Corros. Sci.*, 52: 3033-3041.
- Ali A, Foaud N (2012). Inhibition of Aluminium corrosion in Hydrochloric Acid Solution Using Black Mulberry Extract. *J. Mater. Environ. Sci.*, 3: 917-924.
- Awad M, Metwally M, Soliman S, El-Zomrawy A (2014). Experimental and quantum chemical studies of the effect of poly ethylene glycol as corrosion inhibitors of aluminum surface. *J. Indust. Eng. Chem.*, 20: 796-808.
- Bentiss F, Traisnel M, Gengembre L, Lagrenée M (1999). A new triazole derivative as inhibitor of the acid corrosion of mild steel: electrochemical studies, weight loss determination, SEM and XPS. *Appl. surf. sci.*, 152: 237-249.
- Clark S, Segall M, Pickard C, Hasnip P, Probert M, Refson K, Payne M (2009). *Materials Studio CASTEP*, version 5.0. Accelrys software Inc., San Diego.
- Dugdale I, Cotton J (1963). An electrochemical investigation on the prevention of staining of copper by benzotriazole. *Corros. Sci.*, 3: 69-74.
- El Haleem SA, El Wanees SA, E. El Aal EA, Farouk A (2013). Factors affecting the corrosion behaviour of aluminium in acid solutions. I. Nitrogen and/or sulphur-containing organic compounds as corrosion inhibitors for Al in HCl solutions." *Corros. Sci.*, 68: 1-13.
- El-Deeb M, Sayyah S, El-Rehim SA, Mohamed S (2013). Corrosion inhibition of aluminum with a series of aniline monomeric surfactants and their analog polymers in 0.5 M HCl solution: Part II: 3-(12-sodiumsulfonate dodecyloxy) aniline and its analog polymer. *Arab. J. Chem.*, in press.
- El-Haddad MN (2013). Chitosan as a green inhibitor for copper corrosion in acidic medium." *Int. j. biol. macromol.*, 55: 142-149.
- El-Haddad MN (2014). Hydroxyethylcellulose used as an eco-friendly inhibitor for 1018 c-steel corrosion in 3.5% NaCl solution. *Carbohydr. polym.*, 112: 595-602.
- El-Haddad MN, Elattar KM (2013). Role of novel oxazocine derivative as corrosion inhibitor for 304 stainless steel in acidic chloride pickling solutions. *Res. Chem. Intermed.*, 39: 3135-3149.
- El-Haddad MN, Fouda AS, Mostafa HA (2013). Corrosion Inhibition of Carbon Steel by New Thiophene Azo Dye Derivatives in Acidic Solution. *J. Mater. Eng. Perf.*, 22: 2277-2287.
- El-Haddad MN, Fouda AS (2013). Corrosion Inhibition and Adsorption Behavior of Some Azo Dye Derivatives on Carbon Steel in Acidic Medium: Synergistic Effect of Halide Ions. *Chem. Eng. Comm.*, 200: 1366-1393.
- El-Haddad MN, Fouda AS (2013). Corrosion inhibition effect and adsorption of aniline derivatives on QD36 steel surface in acidic solution. *Prot. Met. Phys. Chem. Surf.*, 49(6): 753-762.
- El-Sayed AR, Mohran HS, El-Lateef HMA (2010). The inhibition effect of 2, 4, 6-tris (2-pyridyl)-1, 3, 5-triazine on corrosion of tin, indium and tin-indium alloys in hydrochloric acid solution. *Corros. Sci.*, 52: 1976-1984.
- Fares, MM, Maayta A, Al-Mustafa JA (2012). Corrosion inhibition of iota-carrageenan natural polymer on aluminum in presence of zwitterion mediator in HCl media. *Corros. Sci.*, 65: 223-230.
- Fouda AS, El-Haddad MN, Abdallah YM (2013). Septazole: Antibacterial Drug as a Green Corrosion Inhibitor for Copper in Hydrochloric Acid Solutions. *International Journal of Innovative Research in Science, Engineering and Technology*, 2: 7073-7085.
- Hosseini M, Mertens SF, Arshadi MR (2003). Synergism and antagonism in mild steel corrosion inhibition by sodium dodecylbenzenesulphonate and hexamethylenetetramine. *Corros. Sci.*, 45: 1473-1489.
- Khadom AA, Yaro AS, Kadhum AAH (2010). Adsorption

- mechanism of benzotriazole for corrosion inhibition of copper-nickel alloy in hydrochloric acid. *J. Chil. Chem. Soc.*, 55: 150-152.
- Lagrene M, Mernari B, Bouanis M, Traisnel M, Bentiss F (2002). Study of the mechanism and inhibiting efficiency of 3, 5-bis (4-methylthiophenyl)-4H-1, 2, 4-triazole on mild steel corrosion in acidic media. *Corros. Sci.*, 44: 573-588.
- Larabi L, Harek Y, Traisnel M, Mansri A (2004). Synergistic influence of poly (4-vinylpyridine) and potassium iodide on inhibition of corrosion of mild steel in 1M HCl. *J. Appl. Electrochem.*, 34: 833-839.
- Lee C, Yang W, Parr RG (1988). Development of the Colle-Salvetti correlation-energy formula into a functional of the electron density. *Physical review B*, 37: 785-789.
- Li X, Deng S, Fu H, Li T (2009). Adsorption and inhibition effect of 6-benzylaminopurine on cold rolled steel in 1.0 M HCl. *Electrochim. Acta*, 54: 4089-4098.
- Li X, Deng S, Xie X (2014). Experimental and theoretical study on corrosion inhibition of o-phenanthroline for aluminum in HCl solution. *Journal of the Taiwan Institute of Chemical Engineers*, 45: 1865-1875.
- Li X, Deng S, Xie X (2014). Experimental and theoretical study on corrosion inhibition of oxime compounds for aluminium in HCl solution. *Corros. Sci.*, 81: 162-175.
- Manivel A, Ramkumar S, Wu JJ, Asiri AM, Anandan S (2014). Exploration of (S)-4, 5, 6, 7-tetrahydrobenzo [d] thiazole-2, 6-diamine as feasible corrosion inhibitor for mild steel in acidic media. *J. Environ. Chem. Eng.*, 2: 463-470.
- Manohar D, Noeline B, Anirudhan T (2006). Adsorption performance of Al-pillared bentonite clay for the removal of cobalt (II) from aqueous phase. *Appl. Clay Sci.*, 1: 194-206.
- Muralidharan S, Phani K, Pitchumani S, Ravichandran S, Iyer S (1995). Polyamino-benzoquinone polymers: a new class of corrosion inhibitors for mild steel. *J. Electrochem. Soc.*, 142: 1478-1483.
- Noor EA (2009). Potential of aqueous extract of Hibiscus sabdariffa leaves for inhibiting the corrosion of aluminum in alkaline solutions. *J. appl. electrochem.*, 39: 1465-1475.
- Obot IB, Ebenso EE, Kabanda MM (2013). Metronidazole as environmentally safe corrosion inhibitor for mild steel in 0.5 M HCl: experimental and theoretical investigation. *J. Environ. Chem. Eng.*, 1: 431-439.
- Obot I B, Obi-Egbedi N, Umoren S (2009). The synergistic inhibitive effect and some quantum chemical parameters of 2, 3-diaminonaphthalene and iodide ions on the hydrochloric acid corrosion of aluminium. *Corros. Sci.*, 51: 276-282.
- Rethinnagiri V, Jeyaprakash P, Arunkumar M, Maheswaran V, Madhiyalagan A (2012). Investigation and inhibition of aluminium corrosion in hydrochloric acid solutions by organic compound. *Adv. Appl. Sci. Res.*, 3: 1718-1726.
- Şafak S, Duran B, Yurt A, Türkoğlu G (2012). Schiff bases as corrosion inhibitor for aluminium in HCl solution. *Corros. Sci.*, 54: 251-259.
- Sastri VS, Ghali E, Elboujdaini M (2007). Corrosion prevention and protection: practical solutions, John Wiley & Sons, ISBN 978-0-470-02402-7, Chichester, England,
- Yurt A, Ulutas S, Dal H(2006). Electrochemical and theoretical investigation on the corrosion of aluminium in acidic solution containing some Schiff bases. *Appl. Surf. Sci.*, 253: 919-925.